Submitted for consideration in the special issue on 3D Cell Biology:

Cell polarity defines three distinct domains in pancreatic beta cells.

Wan J Gan[1,2], Michael Zavortink[1], Christine Ludick[1], Rachel Templin[3], Robyn Webb[3], Richard Webb[3], Wei Ma[2], Philip Poronnik[4], , Robert G. Parton[3,5], Herbert Y Gaisano[6], Annette M. Shewan[7], and Peter Thorn[1,2*]

[1]School of Biomedical Sciences, University of Queensland, St Lucia, QLD 4072, Australia.
[2]Charles Perkins Centre, John Hopkins Drive, University of Sydney, Camperdown, NSW, Australia
[3]Centre for Microscopy and Microanalysis, University of Queensland, St Lucia, QLD 4072, Australia.
[4]Department of Physiology, School of Medical Sciences, The University of Sydney, Camperdown, NSW, Australia
[5]Institute for Molecular Bioscience, University of Queensland, St Lucia, QLD 4072, Australia.
[6]Department of Medicine, University of Toronto, Toronto, Ontario, Canada.
[7]School of Chemistry and Molecular Biosciences, University of Queensland, St Lucia, QLD 4072, Australia.

[*]Author for correspondence: p.thorn@sydney.edu.au

Keywords: insulin, polarity, islet, diabetes

Summary Statement

3D imaging methods identify three structural and functional domains within beta cells in islets; apical, lateral and basal.

ABSTRACT

The structural organisation of pancreatic beta cells in the islets of Langerhans is relatively unknown. Here, using 3D two-photon, 3D confocal and 3D block-face serial electron microscopy, we demonstrate a consistent *in situ* polarisation of beta cells and define three distinct cell-surface domains. An apical domain located at the vascular apogee of beta cells, defined by the location of PAR-3 and ZO-1, delineates an extracellular space into which adjacent beta cells project their primary cilia. A separate lateral domain, is enriched in scribble and Dlg, and colocalises with E-cadherin and GLUT2. Finally, a distinct basal domain, where the beta cells contact the islet vasculature, is enriched in synaptic scaffold proteins such as liprin. This 3D analysis of beta cells within intact islets, and the definition of distinct domains, provides new insights in to understanding beta cell structure and function.

Journal of Cell Science • Advance article

INTRODUCTION

Cell polarity is established in response to external cues and drives cell orientation and regional specialisations that are essential for cell function (Roignot et al., 2013; Yu et al., 2005). Apical-basal polarity determinants define intracellular domains and create membrane segregation (Bryant et al., 2010). These domains are then the target for the location and trafficking (Cao et al., 2012; Mellman and Nelson, 2008) of specific proteins that in turn are critical for function. Perhaps the best known class of cells that are polarised are epithelial cells. For example, in pancreatic acinar cells, apical location of the exocytic machinery (Gaisano et al., 1996) and calcium release apparatus (Thorn et al., 1993) are essential for the unidirectional secretion of digestive enzymes and fluid in to the pancreatic duct.

In the case of epithelial cells the key molecular mechanisms that establish polarity are understood in terms of polarity determinant complexes that include a tight junctional complex of PAR-3/PAR-6/aPKC (Goldstein and Macara, 2007) and a basal complex of Dlg/Lgl/Scribble (Humbert et al., 2003). However, there are many cell types, such as endocrine cells, where functions are located in distinct cellular regions (Moser and Neher, 1997), but where it is unknown if these specialisations are located by mechanisms of polarity. A good example is the insulin-secreting pancreatic beta cell. It is known that the main glucose uptake transporter, GLUT2 is located on the lateral membrane between the cells (Orci et al., 1989). Evidence also indicates that insulin secretion selectively occurs at the vascular face of the beta cells (Low et al., 2014). These segregated functions imply beta cell polarity and work on polarity pathways, such as LKB1 (Fu et al., 2009; Granot et al., 2009; Kone et al., 2014), or viral budding (Lombardi et al., 1985) support this idea. However, islets of Langerhans are a compact mass of thousands of cells and do not have obvious physical boundaries and domains, such as lumens that are found in epithelial tissues. As such, it is unclear whether beta cells have a consistent orientation in the islet and unknown if they possess the classical polarity determinants that might underpin regional specialisations.

Here we have used a pancreatic slice preparation that maintains the native structural organisation of the islets (Marciniak et al., 2014). We have imaged in three dimensions, using three distinct methods; live-cell two photon microscopy, immunofluorescence confocal microscopy and finally, serial block face electron microscopy. Together, these methods provide new insights on the *in situ* organisation of beta cells and show that they are consistently orientated with respect to the vasculature with polarity determinants that define three distinct domains.

RESULTS

Beta cells possess at least two distinct functional domains.

Most of the islet volume consists of endocrine cells packed in close contact with each other, but most endocrine cells also make contact with the capillary blood vessels (Weir and Bonner-weir, 1990). The contact points of the beta cells to the vasculature have been proposed, based on the distribution of insulin granules, as the site of insulin granule exocytosis (Bonner-Weir, 1988). We provide direct functional evidence for this, using 3D live-cell imaging of glucose-induced insulin granule exocytosis, and employing a two-photon granule fusion assay (Fig. 1A, (Low et al., 2013;

Low et al., 2014)). Insulin granule fusion, in response to glucose stimulation, is strongly biased towards the blood vessels, in this case stained with isolectin B4 (Fig. 1B). To further characterise these beta cell–vascular contact points we used 3D electron microscopy, employing serial block-face sectioning of intact fixed mouse islets (Fig. 1B). All cells made one point of contact and many (11/19 cells in this block) had two points of contact with the vasculature. The total area of this contact is proportionately small compared to the total cell membrane area of the beta cells (vascular contact area is 7.9+/-3.8 %, n=19 cells, Fig. 1C).

As well as being the domain of targeted exocytosis, the regions of beta cells that contact the vasculature are also enriched in synaptic scaffold proteins, like liprin (Fig. 2A,B,C,D and Supplemental Movie 1), as well as other synaptic proteins such as RIM2, ELKS and piccolo (Low et al., 2014). Thus both functional and structural evidence indicate this region as a distinct beta cell domain specialised for secretion. This domain at the vascular face is separate from the distribution of GLUT2, which is on the lateral regions between cells (Fig. 2E,F,G and Supplemental Movie 2). GLUT2 is the main glucose influx pathway in rodents and the segregation of this domain from the secretory domain suggests a hitherto unrecognised importance to the spatial organisation of the stimulus-secretion pathway.

Beta cells show a consistent orientation with respect to the vasculature.

The above data suggest a 3D organisation of beta cells and a consistent spatial relationship with the vasculature of the islet. As an aid to understanding these relationships we have further analysed our immunofluorescence data from islet slices. Firstly, in single planes, we defined three separate plasma membrane domains: (1) the vascular face, identified by the colocalisation with the basement membrane protein laminin, (2) the lateral domains along the sides of the cells (3) the vascular apogee, identified as the region of cell membrane furthest away from the vasculature (Fig. 2C). A linescan analysis across each of these membrane domains, as shown in Fig. 2B, identified the peak fluorescence which, when plotted out, shows an enrichment of liprin at the vascular face, as identified with laminin (Fig. 2C). Secondly, we 3D reconstructed the cell-surface distribution of liprin and laminin using linescans around the cell circumference at each image Z plane, with fluorescence intensity represented as a heatmap (Fig. 2D). Both approaches show that liprin is specifically enriched along the vascular face of the beta cells and demonstrate a consistent orientation of beta cells with respect to the vasculature, suggesting that beta cells are polarised.

We performed a similar analysis for the 3D distribution of GLUT2 and again used laminin as a marker for the vascular face (Fig 2E,F,G). GLUT2 was specifically enriched along the regions away from the vasculature where there are endocrine-endocrine contacts, as shown in the 2D linescans (Fig. 2F) and the 3D cell circumference heatmap (Fig. 2G).

Evidence for a third spatial domain in beta cells.

Recent work has highlighted the importance of primary cilia in beta cell function (Gerdes et al., 2014). Primary cilia are often located in the apical region within a spatial domain defined by tight junctions. We therefore used our methods, in pancreatic slices, to determine if primary cilia and tight junctions in beta cells also have a consistent orientation in the islet. We show that the tight junction protein zona occludens 1 (ZO-1) and acetylated tubulin, as a marker for primary cilia, are present in cells in the islet (Fig. 3A) with both proteins positioned at the vascular apogee (Fig. 3B,C

and Supplemental Movie 3) indicting this region as a likely apical domain. Reanalysis of the electron microscopy data in Fig. 1C confirms that the primary cilia is located away from the two blood vessels (Supplemental Fig. 3A) In total therefore, we suggest the beta cells possess three functionally distinct domains; apical, lateral and basal. Our 3D analysis indicates these domains are consistently orientated with respect to the vasculature and imply an underlying cellular polarity.

Apical polarity determinants define an apical region in the beta cell that is opposite to the vascular face.

If beta cells really are polarised then they might be expected to possess the determinants of polarity that are found in epithelial cells. Using islet slices and immunostaining (Low et al., 2014; Meneghel-Rozzo et al., 2004) we determined if the islet cells possess the classical apical determinant, PAR-3 (Fig. 3D). The images show that PAR-3 is consistently located away from the laminin stained vasculature and is relatively discrete, occupying a small domain of the cells, that contrasts with E-cadherin staining which is enriched along the entire lateral membrane (Fig. 3D and Supplemental Movie 4). Using linescan analysis and domain distribution, as well as 3D circumference heatmap, to quantify the protein locations it is clear that both are excluded from the beta cell vascular face, that E-cadherin is enriched on the lateral domain, and PAR-3 is enriched at the vascular apogee which, given this defining feature, we will now term the apical domain (Fig. 3E,F,H). Fig. 3G, proves that PAR-3 is present in beta cells, which, in these experiments were counter immunostained with insulin.

To increase our spatial resolution of this apical domain we turned again to serial block-face electron microscopy. Using 50 nm thick sections, through a depth of 25 µm, enabled us to identify the orientation and components of the putative apical domain. The region of the vascular apogee shows evidence for contact points of close apposition between beta cells that are consistent with tight junctional links (Fig. 4A, arrow heads) and were used to provide the outline volume of an extracellular apical lumen (yellow, Fig. 4B,C). Projecting in to this lumen are primary cilia that show evidence for centrioles at their bases (Fig. 4A, arrows). Each serial section (Fig. 4B, Supplemental Fig. 1) was then used to produce a reconstructed image, drawn from all the sections within the volume, which shows the vasculature (red) on the left, and a single exemplar cell outlined in mesh (grey) with its nucleus (blue) and cilia from four adjacent beta cells (green, orange, blue and purple) that all project in to the extracellular luminal space (Fig. 4C and Supplemental Movie 5). Together our data indicate that tight junctions and primary cilia define a discrete spatial domain in beta cells that lies opposite to the vasculature.

Basolateral polarity determinants define the lateral regions between beta cells and the vascular face.

Since the above experiments define an apical region away from the vascular face we next set out to determine the presence and location of protein determinants of the basal domain. Immunostaining for either Dlg (Fig. 5A) or scribble (Fig. 5B) showed that these are located around the beta cell membrane, with a particular enrichment along the lateral surfaces (Fig. 5C,F,G and Supplemental Movies 6, 7). We prove, using counter immunostaining that these basal polarity determinants are located in insulin-positive beta cells (Fig. 5D,E) and conclude that these basal

determinants provide further evidence that beta cells are systematically orientated with respect to the vasculature and can be considered as polarised cells.

This polar organisation of beta cells within islets is conserved in humans. Immunostaining of human islets showed that PAR-3 is located in the vascular apogee of insulin-containing beta cells; consistent with the mouse data (Supplemental Fig. 2A). We also show that scribble is located in the lateral and basal regions of insulin-containing beta cells (Supplemental Fig. 2C). Quantitative assessment of the distribution of these proteins (Supplemental Fig. 2B) shows a similar distribution to that of beta cells in the mouse islets.

DISCUSSION

Here we show that pancreatic beta cells maintain a consistent orientation with respect to the islet capillaries that is defined by apical and basal regions and the positioning of polarity determinants, like PAR-3 and scribble. Our approach employs a pancreatic slice method (Marciniak et al., 2014) which preserves the native islet organisation; unlike the more widely used islet cultures which show structural changes, like an increase in tight junctions that can be induced by the enzyme treatments (Intveld et al., 1984) and loss of endothelial cells (Lukinius et al., 1995). Our pancreatic slice method is rapid and uses enzyme inhibitors and is therefore likely to closely reflect the native organisation and expression of tight junctional proteins.

Subsequent imaging with either confocal or block-face serial electron microscopy has enabled us to build up a comprehensive picture of the 3D arrangement of beta cells within the islet. We quantify the 3D spatial distribution of polarity determinants to demonstrate three distinct domains in beta cells. Firstly, an apical region, identified by enrichment of PAR-3 and ZO-1, that encompasses an extracellular “lumen” in to which project primary cilia. Secondly, a lateral region enriched with scribble and Dlg that co-localizes with the GLUT2 transporter. And, finally, a basal region where beta cells contact the vasculature and show enrichment of synaptic scaffold proteins like liprin. The compartmentalised location of these structural and functional proteins suggests that polarity regulates beta cell function.

Beta cell polarity defines three distinct domains:

We firstly identify a distinct apical domain in beta cells.

Our data show a supra-cellular organisation that links tight junctions from one cell to another, which together, circumscribe an extracellular volume in to which primary cilia project from a number of adjoining beta cells (Fig. 4). Given the sensory function of primary cilia (Singla and Reiter, 2006) and recent work that suggests they are the site of enrichment of insulin receptors (Gerdes et al., 2014), this definition of a new domain within the islets has widespread implications for autocrine and paracrine signalling.

Secondly we identify a lateral domain.

Our data show a consistent local enrichment of scribble and Dlg along the lateral membrane that lies between beta cells and separates the apical region at the vascular apogee from the basal region where the beta cells contact the vasculature. This is also the region of enrichment of E-

cadherin and GLUT-2. The significance of separating a region of glucose uptake, away from the vasculature, where insulin secretion occurs (Low et al., 2014) adds a new level of insight in to the stimulus-secretion coupling cascade in beta cells and is likely to be functionally significant in the control of insulin secretion.

Finally we identify a distinct basal region that contacts the vasculature.

We suggest that the most significant interaction is between the beta cells and the basement membrane that is secreted by the endothelial cells. Our imaging shows that the basolateral determinants, Dlg and Scribble, are present in this region, although, as in epithelial cells, they are less abundant than along the lateral domain. Past work has shown that this is the region where the majority of insulin granule exocytosis occurs which would therefore target insulin delivery in to the blood stream (Low et al., 2014). The spatial segregation of this "secretory" region from the lateral and apical domains, once again, provides significant new insights in to beta cell function and islet structure. For example, targeting insulin secretion in to the vasculature spatially segregates insulin detection at the cilia which would minimise autocrine communication and make the beta cells responsive to circulating insulin; as predicted in a recent modelling paper (Wang et al., 2013).

Comparison with past work: apical and lateral regions.

We suggest that the luminal extracellular space we identify here is the same as the previously identified canaliculi (Yamamoto and Kataoka, 1984). The original description, using electron microscopy, showed canaliculi contain microvilli and cilia and are bordered by tight junctions (Yamamoto and Kataoka, 1984). The co-localisation of ZO-1, acetylated tubulin and PAR-3 we now show is good evidence that this apical domain is defining the same extracellular space as the previously described canaliculi. This has interesting implications for beta cell function since we are now making a spatial distinction between this apical domain which forms a discrete region and the much larger lateral surface.

In our model both the apical domain and lateral domain must have functional continuity with the blood. For the apical region this is needed for sensing of insulin, and maybe other factors, by the cilia and in the lateral region it is needed for the uptake of glucose by GLUT2. We suggest that the tight junctions, which are known to be labile (Intveld et al., 1984), might be modulated by different physiological inputs, such as glucose (Orci, 1976) and therefore could be functionally important in selectively restricting diffusional access to the apical lumen.

Our immunostaining of GLUT2 is consistent with a previous report showing it occupies the large lateral surfaces (Thorens et al., 1990). However, other work suggests the GLUT2 transporter is enriched on microvilli (Orci et al., 1989) which, in the context of our model, would place it in the apical domain. However, Orci's work shows GLUT2 is also present on the flat membrane lying between the cells, a region we would classify as lateral. Since this lateral region is much more extensive than the apical it could be functionally dominant for the sensing of glucose. Further work is needed to clarify this point since the specific site of enrichment, of functionally important GLUT2 transporters, in the apical or lateral domains has major implications for the control of beta cell behaviour.

Recent work on cultured islets, suggests F-actin enrichment along cell "edges" between beta cells (Geron et al., 2015) that was also enriched in proteins, such GLUT2 or SNAP25. Our data

here, and elsewhere (Low et al., 2014) argues these proteins are present relatively uniformly across the entire lateral surface of cell-to-cell contacts. The differences might be due to the use of cultured islets vs acute slices; if so the study of any structural reorganisation could give useful insights into the mechanisms that are needed to build beta cell architecture.

Comparison with past work: basal region

Beta cell contacts with the endothelial basement membrane are the site of laminin-integrin interactions that are important for beta cell proliferation (Nikolova et al., 2006). Here we show that this same region contains Dlg and scribble, classical markers for basal domains, and is the site for preferential fusion of insulin granules. Whether insulin secretion can be spatially targeted has been controversial with evidence for (Bokvist et al., 1995; Bonner-Weir, 1988; Paras et al., 2000) and against (Rutter et al., 2006; Takahashi et al., 2002) targeting. Our live-cell 3D imaging, *in situ*, within intact islets, now precisely maps the beta cell to vasculature contacts and provides direct evidence for a strong bias of exocytosis at the vascular face (Fig.1 and (Low et al., 2014)).

The arrangement of beta cells around a capillary has been described as a rosette (Bonner-Weir, 1988). Such rosettes are apparent in some of our images but the 3D complexity of the islet blood vessels means that in many cross sections this organisation is not clear. The seminal paper of Bonner-Weir (Bonner-Weir, 1988) suggested that the majority of beta cells make two points of contact with blood vessels; consistent with our analysis. It is attractive to think that this represents one point of arteriole contact and one point of veniole contact but there is little evidence to support this idea.

Comparison with past work: polarity

Past work has discussed beta cell polarity, in terms of nuclear position and location of cilia (Granot et al., 2009; Kone et al., 2014; Sun et al., 2010). The position of the primary cilia, taken as a proxy for the apical domain, led to the suggestion that the beta cells are more similar to hepatocytes (Granot et al., 2009), with apical regions situated along the lateral surfaces, rather than a classical columnar epithelial organisation where the apical domain is opposite to the basal.

Our 3D analysis now extends our understanding and shows further complexity to beta cell polarity. We show that in terms of area the largest domain of beta cells is the lateral surface formed at endocrine-endocrine cell contacts. Within this lateral surface is a discrete apical domain. The contiguous alignment of apical domains from adjacent cells forms an extracellular lumen. This apical region is positioned at the furthest distance away from the points of vascular contact(s). These sites of vascular contact, we propose, form a distinct basal surface; in this way two points of contact would lead to two basal surfaces. This suggests that beta cells can have multiple basal and apical surfaces embedded within the larger area of the lateral surface. Cartoons representing our proposed cell orientation with respect to the vasculature are shown in Supplemental Fig. 3B. Work in other systems is expanding our understanding of cell polarity to include cell types with multiple apical domains (Denker et al., 2013) perhaps pancreatic beta cell represent another extension of this diversity. Finally, our work indicates that the polar organisation of beta cells we find in the mouse islet is recapitulated with a similar organisation in

the human despite the fact that other significant differences exist between mouse and human islets (Cabrera et al., 2006).

Conclusions

We conclude that beta cells are structurally and functional subdivided into three distinct domains. This cell polarisation spatially separates cell functions and our work provides a framework for future work in to understanding beta cell control. The next stage in exploring beta cell polarity will require further technical advances that enable routine manipulation of beta cells *in situ* and potentially the use of *in vitro* morphogenetic 3D models, such as are used in epithelial cell biology (Cerruti et al., 2013).

MATERIALS AND METHODS

Experimental Solution.

Experiments were performed in Na-rich extracellular solution (in mM: 140NaCl, 5KCl, 1$MgCl_2$, 2.5$CaCl_2$, 5$NaHCO_3$, 5HEPES, glucose) adjusted to pH 7.4 with NaOH.

Islet preparation.

Mice were humanely killed according to local animal ethics procedures (approved by the University of Queensland, Anatomical Biosciences Ethics Committee). Human islet slices were obtained from the Network for Pancreatic Organ Donors with Diabetes (nPOD) tissue bank with cryopreserved tissue sections that were paraformaldehyde fixed and then immunostained following the protocol below.

Islet slices.

Sectioning of unfixed pancreatic tissue was performed as described by Huang et al (Huang et al., 2011). Briefly, after cervical dislocation, the pancreas of 10-12 week old CD1 male mice was injected with 1.9% low melt agarose (UltraPure LMP, invitrogen) in extracellular slice medium (ECSM, 125 mM NaCl, 2.5 mM KCl, 1.25 mM NaH_2PO_4, 26 mM $NaHCO_3$, 2 mM sodium pyruvate, 0.25 mM ascorbic acid, 2mM myo-inositol, 1mM $MgCl_2$, 2mM $CaCl_2$, 6 mM lactic acid and 6 mM glucose at pH 7.4). The common bile duct was clamped at the junction with the duodenum to prevent agarose from entering the small intestine and a 30 gauge needle was used to inject 1-3 mls of 42°C agarose through the bile duct to backfill the pancreas. The pancreas was immediately cooled with ice cold ECSM, removed from the mouse, and immersed in ice cold ECSM in a petri dish. 4 to 6 mM cubes of this tissue were embedded in 4% low melt agarose in ECSM, immersed in 4°C ECSM and sectioned with a Zeiss (Thermo-Fisher) Hyrax V50 vibrating microtome. Sections (90-100 µm thick) were cut with the instrument set at an amplitude of 0.7 and frequency of 95 and a speed of 4 µm/sec and sections containing uncut islets were stored in ECSM (oxygenated by bubbling with 5% carbogen gas and supplemented with 0.1mg/ml trypsin inhibitor (Sigma)) at 4°C, for no longer than 10 minutes, before fixation. Fixation with 4% paraformaldehyde (Sigma-Aldrich) in ECSM was either for 10 minutes (short PFA) or one hour (long PFA) at 20°C. Slices fixed with methanol were rapidly immersed in -20°C methanol and stored in a freezer for one hour. Methanol-fixed slices were rehydrated in ECSM and then PBS. Slices were stored in either PBS or ECSM at 4°C for up to one week before antibody treatment.

Immunofluorescence was performed as described by Meneghel-Rozzo et al (Meneghel-Rozzo et al., 2004). Sections were incubated in block buffer (3% BSA, 0.3% donkey serum, 0.3% Triton X-100) for a minimum of one hour at room temperature followed by primary antibody incubation at 4° C overnight in block buffer. Typically 4-6 slices were incubated in 0.5 ml block buffer in 1 well of a 6 well dish. Sections were washed in PBS (4 changes over 30 minutes) and secondary antibodies (in block buffer) were added for 4-6 hours at 20° C. After washing in PBS, sections were mounted in Prolong Gold anti-fade reagent (Invitrogen) and imaged on an Olympus Fluoview FV1000 confocal microscope using a UPlanSApo 60X 1.35 N.A. oil objective.

The linescan analysis, for example in Fig. 2B, identified the peak fluorescence at, or close to the membrane, that was then averaged to produce the distribution plots shown, for example, in Fig. 2C. The heatmap representations (for example in Fig. 2D) used fluorescence intensities along linescans around the cell circumference at each Z section. The resultant array of fluorescence intensities was then normalised to the brightest region and shown on a blue-yellow-red (fluorescence intensity 0-100%) colour scale.

Serial block-face electron microscopy.

Serial Block-Face Scanning Electron Microscopy (SBFSEM). Pancreatic slices were fixed in 2.5% glutaraldehyde, washed in PBS and double post-fixed by using 2% OsO_4 with 1.5% potassium ferricyanide followed by 1% thiocarbohydrazide and then another 2% OsO_4. Samples were stained overnight with 1% uranyl acetate and then for 1 hour at 60^{o}C in Walton's lead aspartate. They were then serially dehydrated with acetone and then embedded with Durcapan resin and polymerised. Individual islets were cut out of the resin, mounted and then imaged and sectioned using a Zeiss Sigma SEM fitted with a 3View (Gatan, CA, USA) at 2.25kv and 10Pa. The resultant images were analysed using the programme IMOD (Kremer et al., 1996) and 3D reconstructions performed.

Antibodies.

Primary antibodies used for this study were: rat anti-beta1 laminin (Thermo Scientific MAS5-14657), mouse anti-Dlg (BD Transduction Lab 610874), mouse anti-E-cadherin (BD Transduction lab 610181), mouse anti-insulin (Sigma I2018), rabbit anti-PAR-3 (Marck Millipore 07-330) Dgl, scribble and rabbit anti-PPFIA1 (liprin 1α Proteintech 14175-1-AP). All primary antibodies, except the laminin antibody, were diluted 1/200, the anti-laminin antibody was used at 1/500. Secondary antibodies were highly cross absorbed donkey or goat antibodies (Invitrogen) labelled with Alexa 488, Alexa 546 or Alexa 633. All were used at a 1/200 dilution. Where used, DAPI (Sigma, 100 ng/ml final concentration) and Alexa 633 phalloidin (A22284, 2U/ml final concentration, Invitrogen) were added for the last 2 hours of secondary antibody incubation.

Statistical Analyses.

All numerical data are presented as mean ± standard error of the mean. Statistical analysis was performed using Microsoft Excel and GraphPad Prism. Data sets with two groups were subjected to a two-tailed, un-paired Student's t-test. Islets from at least 3 animals were used in each experiment.

Competing Interests

The authors declare no competing or financial interests.

Author Contributions

Wan Gan, Michael Zavortink, Christine Ludick, Rachel Templin, Robyn Webb, Richard Webb all designed and performed the experiments. Philip Poronnik analysed the data. Robert Parton, Herbert Gaisano, Annette Shewan, and Peter Thorn designed the experiments. All authors contributed to the analysis and writing of the manuscript.

Funding

This work was supported by an Australian Research Council Grant DP110100642 (to PT) and National Health and Medical Research Council Grants APP1002520 and APP1059426 (to PT and HYG) and APP1037320 (to RGP) and a Diabetes Australia grant Y15G-THOP (to PT).

This research was performed with the support of the Network for Pancreatic Organ Donors with Diabetes (nPOD), a collaborative type 1 diabetes research project sponsored by JDRF. Organ Procurement Organizations (OPO) partnering with nPOD to provide research resources are listed at http://www.jdrfnpod.org/for-partners/npod-partners/

Figures

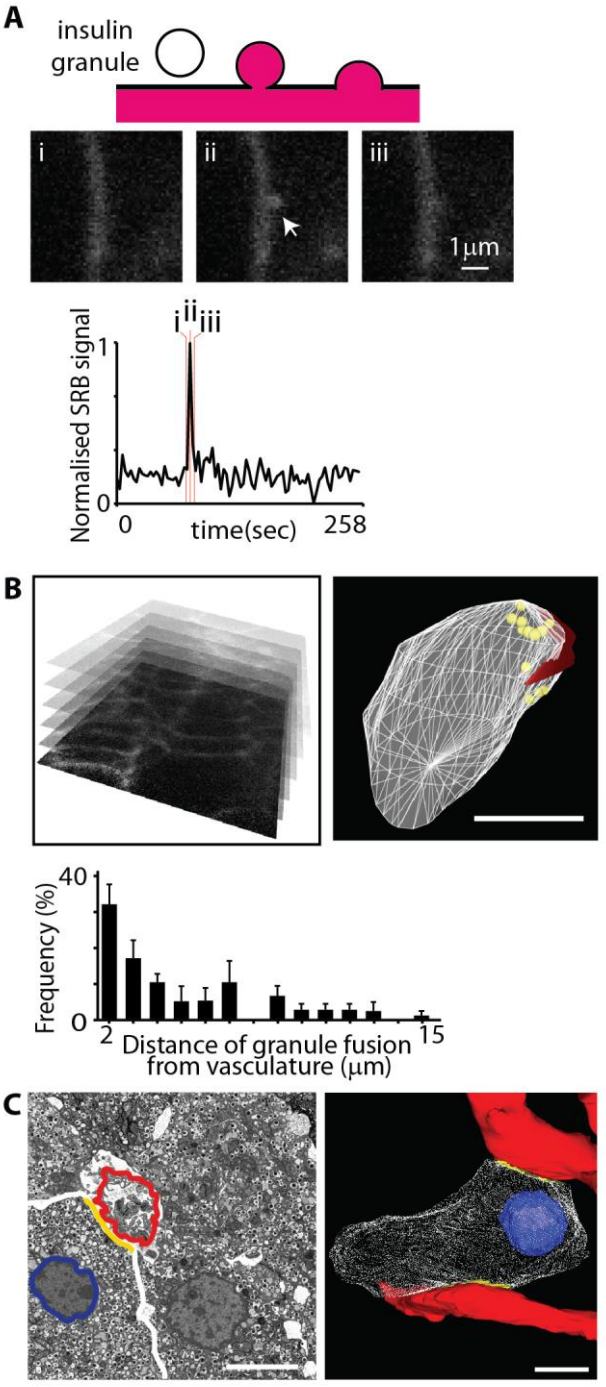

Fig. 1**. Beta cells are arranged with a consistent orientation with respect to the islet blood vessels.** (A) Live-cell, 3D two-photon microscopy tracks the rapid influx of sulforhodamine B (SRB) dye into fusing granules, previously characterised as insulin-containing granules, in response to a 15 mM glucose stimulus (Low et al., 2013). An individual fusion event is shown at three times (i, ii, iii) with the fluorescence intensity over time, within a region of interest centred over the granule,

showing a sharp peak and rapid decay. (B) Data collected in 3D, with 2 µm between each section, shows the location of each granule fusion event as yellow circles. The basement membrane marker, isolectin B4 (shown in red) identifies the region of the beta cell adjoining the vasculature. 3D analysis of the distribution of granule fusion distances shows a strong bias towards the vasculature. (C) Serial block face scanning electron microscopy (single image from the stack shown on the left) identified the 3D relationships between the blood vessels (red) and beta cells with the contact points (yellow) defining a small membrane domain (3D reconstruction shown on the right). Total of 19 cells in this volume, 8 cells make single contact with vasculature, 11 cells make 2 points of contact. Scale bars 5 µm.

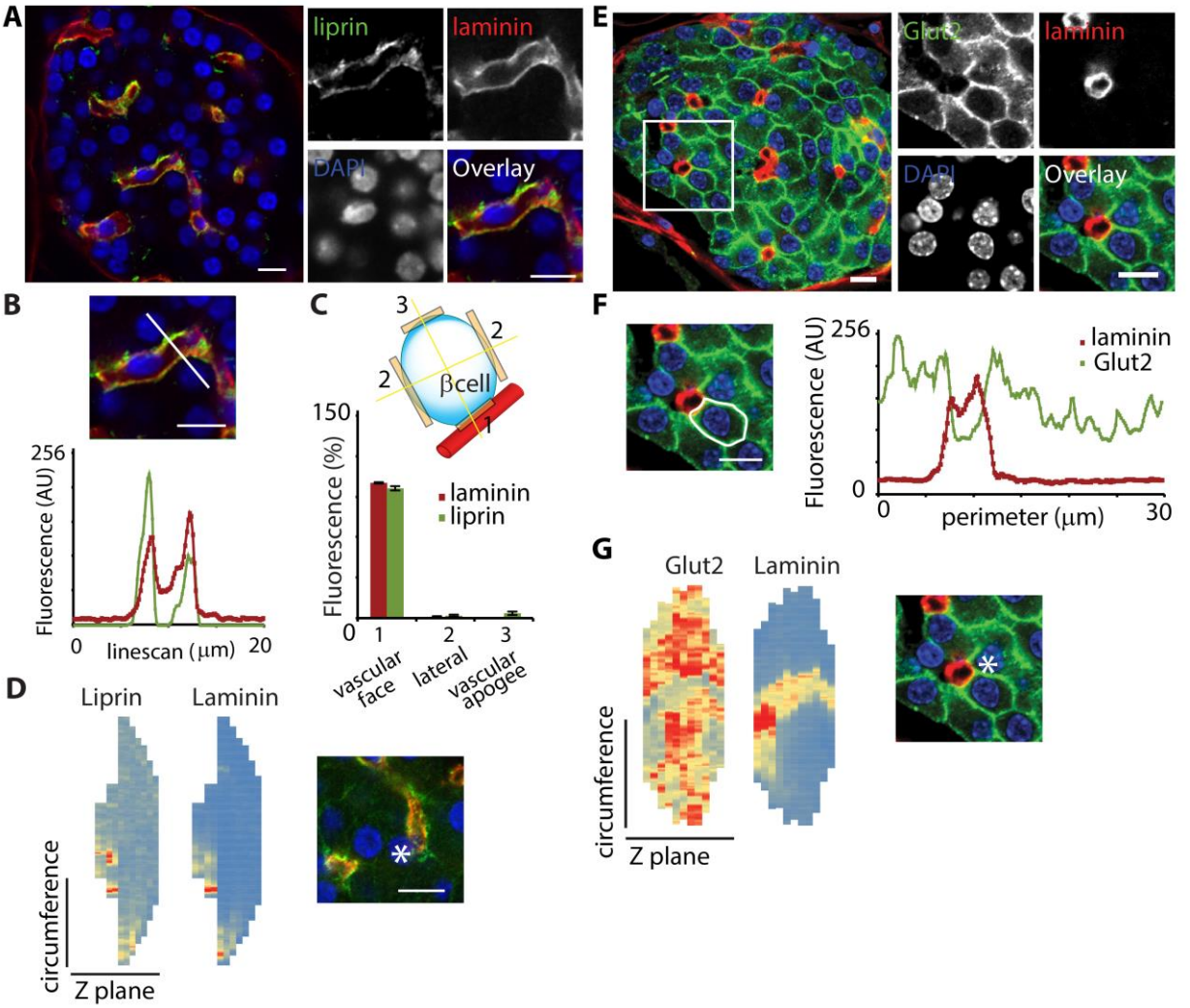

Fig. 2. **Enrichment of the synaptic protein, liprin, and GLUT2 in specific and distinct domains.** (A) Immunofluorescence shows the synaptic scaffold protein liprin (green) is enriched along the vascular face of beta cells (labelled with laminin, red). (B) A linescan drawn across a blood vessel shows the coincidence of liprin and laminin location; previous work has proved liprin is expressed in beta cells (Low et al., 2014). (C) A schematic of a beta cell illustrates a division of the cell membrane into 3 domains. Linescan analysis of the peak fluorescence in each domain, quantitatively identifies enrichment of liprin at the vascular domain (n=14 cells within 1 islet, representative of the distribution in islets from 6 animals). (D) heatmap representation (blue is low fluorescence, red is high fluorescence) of liprin and laminin distribution, using fluorescence intensities along cell circumference linescans at each Z stack, shows coincident enrichment of both proteins at the vascular face of the beta cell. (E,F) Immunofluorescence of GLUT2 (green) shows enrichment along the lateral regions away from the vasculature immunostained with laminin (red). (G) A heatmap representation, using cell circumference linescan analysis at each Z stack, shows that GLUT2 is widespread across the cell-surface, but laminin has a relatively discrete enrichment. Scale bars 10 μm.

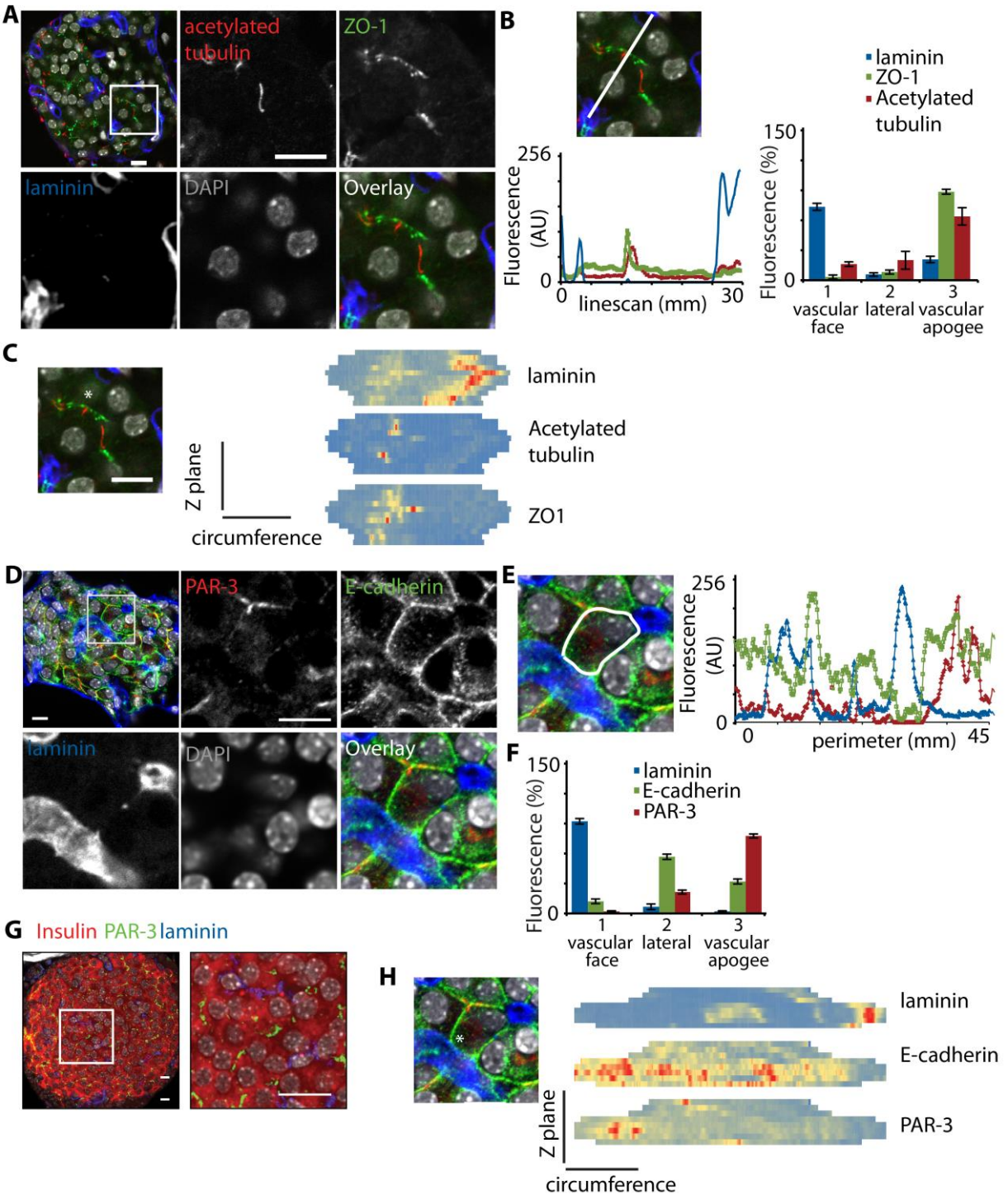

Fig. 3**. Identification and characterisation of an apical domain in beta cells.** (A) Immunostaining of acetylated tubulin (as a marker for primary cilia, red) and ZO-1 (green) shows enrichment at the pole of the beta cell that lies away from the vasculature (labelled with laminin, blue). (B) Linescan and distribution analysis demonstrates the enrichment of acetylated tubulin and ZO-1 in domain 3, at the vascular apogee (data from 13 cells from 2 islets, representative of ZO-1 repeated in islets from 6 animals, tubulin repeated in islets from 8 animals). (C) A heatmap representation, using cell circumference linescan analysis at each Z stack, shows ZO-1 and acetylated tubulin have a coincident enrichment at the opposite side of the cell to laminin. (D) The apical determinant, PAR-

3 (red) is enriched at the pole of beta cells that lies away from the vasculature (labelled with laminin, blue) and contrasts with the distribution of E-cadherin (green) which is found along the lateral membrane domains. Scale bars 10 µm. (E) A linescan drawn around the perimeter of a single cell (white line) shows the relative distribution of these proteins. (F) This is further quantified with a linescan analysis of immunoflourescence across the membrane domains of the beta cells which shows E-cadherin enriched on the lateral membrane and PAR-3 at the vascular apogee (n=13 cells from 1 islet, representative of PAR-3 repeated in islets from 8 animals, E-cadherin repeated in islets from 4 animals) (G) Immunolocalisation of PAR-3 (green) with insulin (red) in whole islets (left) and magnified image (right). (H) A heatmap representation, using cell circumference linescan analysis at each Z stack, shows the widespread distribution of E-cadherin and the enrichment of PAR3 that is positioned away from the enrichment of laminin. Scale bars 10 µm.

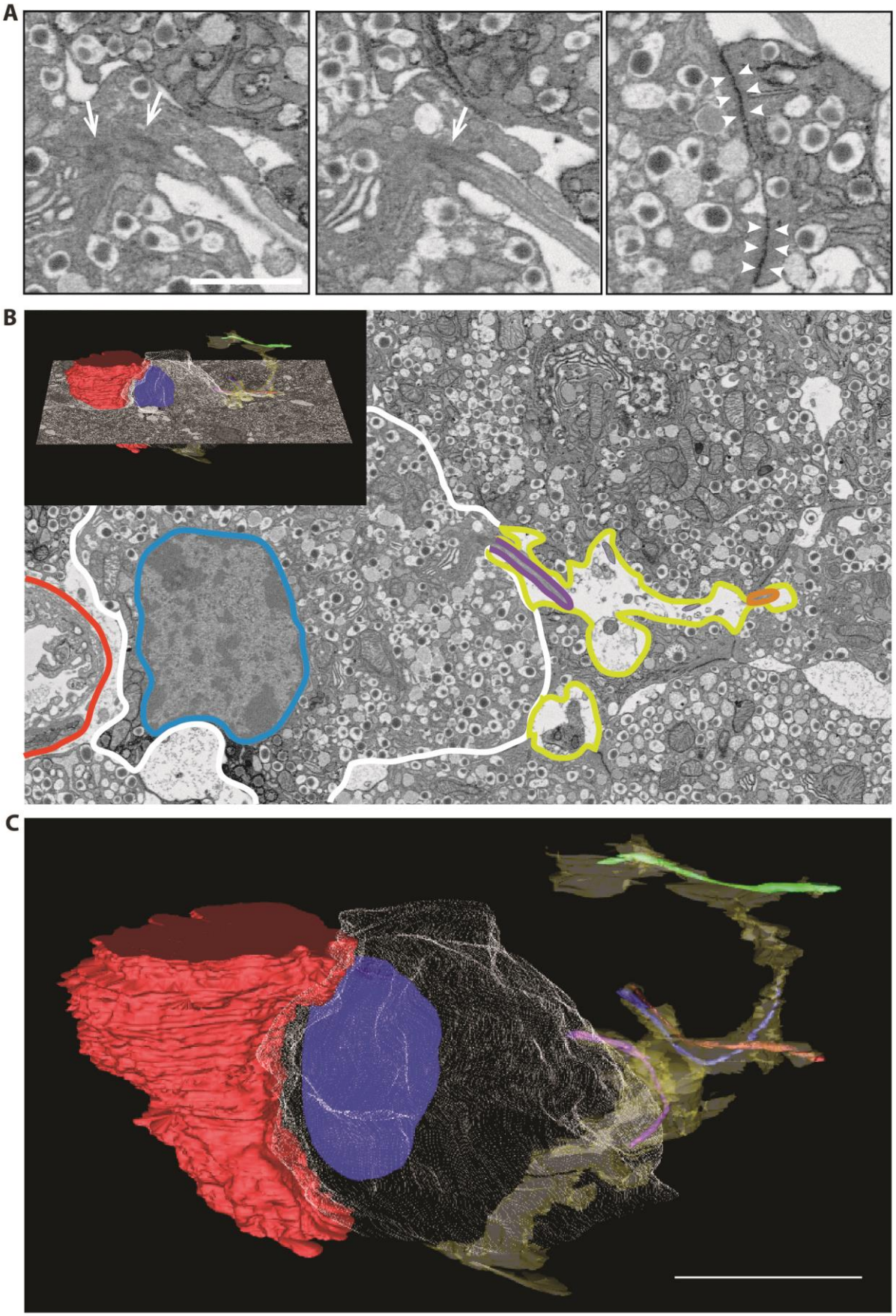

Fig. 4**. Serial electron microscopy defines an apical domain and supra-cellular luminal volume.** (A) Enlarged regions from single electron microscopy sections shows the centrioles (arrows) at the base of an example primary cilia and the putative tight junctions (arrow heads). (B) 50 nm serial sections were then used to construct a model in IMOD that highlights a single beta cell (mesh outline, blue nucleus) within an islet. This cell contacts the blood capillary (red) on the left. Regions of close apposition between adjacent beta cells, consistent with tight junctions were used to outline a contiguous extracellular space (yellow outline) suggestive of a discrete luminal compartment in which adjacent beta cells also place their primary cilia (green, blue orange and purple). (C) The full-depth model of the single cell shows its relationship to the vasculature and the luminal space. Blood capillary: red, Beta cell: white, Nucleus: blue, extracellular luminal space: yellow, Primary cilia: green, blue, orange and purple lines.

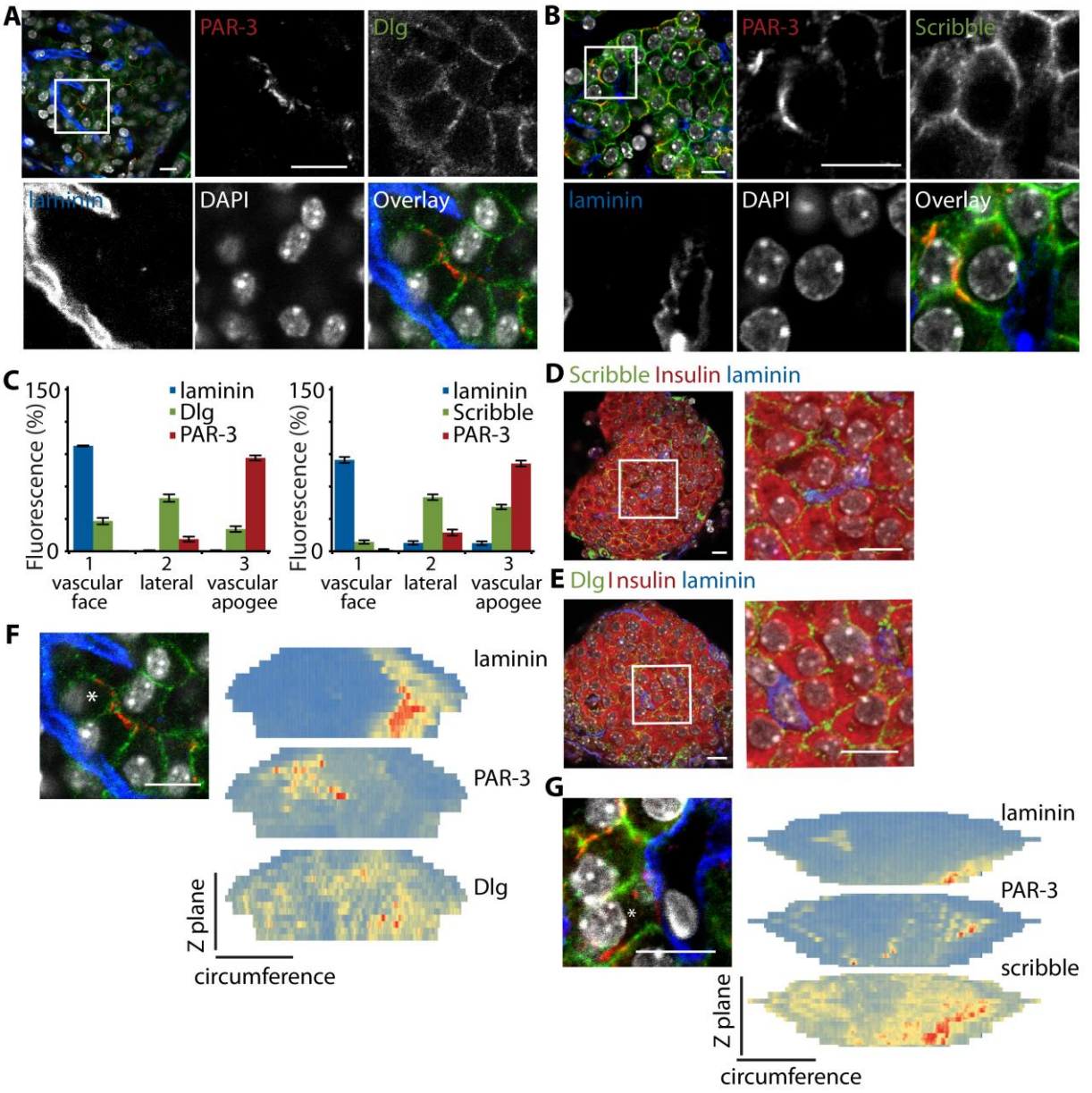

Fig. 5. **Identification of the basal region of beta cells using Dlg and scribble.** (A,B) Immunostaining with PAR-3 and Dlg or scribble shows a predominantly lateral location of Dlg and scribble. (C) This was quantitatively confirmed, using linescan analysis and identifies relative enrichment of both Dlg and scribble in the lateral domain. Counter immunostaining for PAR-3 showed the characteristic enrichment in the vascular apogee, as before (Dlg: n=20 cells from 3 islets, scribble: n=15 cells from 2 islets, representative of Dlg repeated in islets from 4 animals, scribble repeated in islets from 7 animals). (D, E) Co-immunolocalisation of scribble or Dlg (both green) with insulin (red) in whole islets and magnified images. (F,G) heatmap representations, using cell circumference linescan analysis at each Z stack, shows the discrete enrichment of laminin (identifying the vascular face) is separated from the enrichment of PAR-3 (apical region) and that both Dlg and scribble have a relatively widespread location across the cell. Scale bars 10 µm.

REFERENCES

Bokvist, K., Eliasson, L., Ammala, C., Renstrom, E. and Rorsman, P. (1995). Colocalization of L-type Ca2+ channels and insulin-containing secretory granules and its significance for the initiation of exocytosis in mouse pancreatic beta-cells. *Embo Journal* **14**, 50-57.

Bonner-Weir, S. (1988). Morphological evidence for pancreatic polarity of beta cell within islets of Langerhans. *Diabetes* **37**, 616-621.

Bryant, D. M., Datta, A., Rodriguez-Fraticelli, A. E., Peranen, J., Martin-Belmonte, F. and Mostov, K. E. (2010). A molecular network for de novo generation of the apical surface and lumen. *Nature Cell Biology* **12**, 1035-U24.

Cabrera, O., Berman, D. M., Kenyon, N. S., Ricordi, C., Berggrern, P. O. and Caicedo, A. (2006). The unique cytoarchitecture of human pancreatic islets has implications for islet cell function. *Proceedings of the National Academy of Sciences of the United States of America* **103**, 2334-2339.

Cao, X. W., Surma, M. A. and Simons, K. (2012). Polarized sorting and trafficking in epithelial cells. *Cell Research* **22**, 793-805.

Cerruti, B., Puliafito, A., Shewan, A. M., Yu, W., Combes, A. N., Little, M. H., Chianale, F., Primo, L., Serini, G., Mostov, K. E. et al. (2013). Polarity, cell division, and out-of-equilibrium dynamics control the growth of epithelial structures. *Journal of Cell Biology* **203**, 359-372.

Denker, E., Bocina, I. and Jiang, D. (2013). Tubulogenesis in a simple cell cord requires the formation of bi-apical cells through two discrete Par domains. *Development* **140**, 2985-2996.

Fu, A., Ng, A. C.-H., Depatie, C., Wijesekara, N., He, Y., Wang, G.-S., Bardeesy, N., Scott, F. W., Touyz, R. M., Wheeler, M. B. et al. (2009). Loss of Lkb1 in Adult beta Cells Increases beta Cell Mass and Enhances Glucose Tolerance in Mice. *Cell Metabolism* **10**, 285-295.

Gaisano, H. Y., Ghai, M., Malkus, P. N., Sheu, L., Bouquillon, A., Bennett, M. K. and Trimble, W. S. (1996). Distinct cellular locations of the syntaxin family of proteins in rat pancreatic acinar cells. *Molecular Biology of the Cell* **7**, 2019-2027.

Gerdes, J. M., Christou-Savina, S., Xiong, Y., Moede, T., Moruzzi, N., Karlsson-Edlund, P., Leibiger, B., Leibiger, I. B., Ostenson, C. G., Beales, P. L. et al. (2014). Ciliary dysfunction impairs beta-cell insulin secretion and promotes development of type 2 diabetes in rodents. *Nature Communications* **5**.

Geron, E., Boura-Halfon, S., Schejter, E. D. and Shilo, B.-Z. (2015). The Edges of Pancreatic Islet beta Cells Constitute Adhesive and Signaling Microdomains. *Cell Reports* **10**, 317-325.

Goldstein, B. and Macara, I. G. (2007). The PAR proteins: Fundamental players in animal cell polarization. *Developmental Cell* **13**, 609-622.

Granot, Z., Swisa, A., Magenheim, J., Stolovich-Rain, M., Fujimoto, W., Manduchi, E., Miki, T., Lennerz, J. K., Stoeckert, C. J., Meyuhas, O. et al. (2009). LKB1 Regulates Pancreatic beta Cell Size, Polarity, and Function. *Cell Metabolism* **10**, 296-308.

Huang, Y. C., Rupnik, M. and Gaisano, H. Y. (2011). Unperturbed islet alpha-cell function examined in mouse pancreas tissue slices. *Journal of Physiology-London* **589**, 395-408.

Humbert, P., Russell, S. and Richardson, H. (2003). Dlg, Scribble and Lgl in cell polarity, cell proliferation and cancer. *Bioessays* **25**, 542-553.

Intveld, P. A., Pipeleers, D. G. and Gepts, W. (1984). Evidence against the presence of tight junctions in normal endocrine pancreas. *Diabetes* **33**, 101-104.

Kone, M., Pullen, T. J., Sun, G., Ibberson, M., Martinez-Sanchez, A., Sayers, S., Nguyen-Tu, M.-S., Kantor, C., Swisa, A., Dor, Y. et al. (2014). LKB1 and AMPK differentially regulate pancreatic β-cell identity. *The FASEB Journal* **28**, 4972-4985.

Kremer, J. R., Mastronarde, D. N. and McIntosh, J. R. (1996). Computer visualization of three-dimensional image data using IMOD. *Journal of Structural Biology* **116**, 71-76.

Lombardi, T., Montesano, R., Wohlwend, A., Amherdt, M., Vassalli, J. D. and Orci, L. (1985). Evidence for polarization of plasma-membrane domains in pancreatic endocrine-cells. *Nature* **313**, 694-696.

Low, J. T., Mitchell, J. M., Do, O. H., Bax, J., Rawlings, A., Zavortink, M., Morgan, G., Parton, R. G., Gaisano, H. Y. and Thorn, P. (2013). Glucose principally regulates insulin secretion in mouse islets by controlling the numbers of granule fusion events per cell. *Diabetologia* **56**, 2629-2637.

Low, J. T., Zavortink, M., Mitchell, J. M., Gan, W. J., Do, O. H., Schwiening, C. J., Gaisano, H. Y. and Thorn, P. (2014). Insulin secretion from beta cells in intact mouse islets is targeted towards the vasculature. *Diabetologia* **57**, 1655-1663.

Lukinius, A., Jansson, L. and Korsgren, O. (1995). Ultrastructural evidence for blood microvessels devoid of an endothelial-cell lining in transplanted pancreatic-islets. *American Journal of Pathology* **146**, 429-435.

Marciniak, A., Cohrs, C. M., Tsata, V., Chouinard, J. A., Selck, C., Stertmann, J., Reichelt, S., Rose, T., Ehehalt, F., Weitz, J. et al. (2014). Using pancreas tissue slices for in situ studies of islet of Langerhans and acinar cell biology. *Nat. Protocols* **9**, 2809-2822.

Mellman, I. and Nelson, W. J. (2008). Coordinated protein sorting, targeting and distribution in polarized cells. *Nature Reviews Molecular Cell Biology* **9**, 833-845.

Meneghel-Rozzo, T., Rozzo, A., Poppi, L. and Rupnik, M. (2004). In vivo and in vitro development of mouse pancreatic beta-cells in organotypic slices. *Cell and Tissue Research* **316**, 295-303.

Moser, T. and Neher, E. (1997). Rapid exocytosis in single chromaffin cells recorded from mouse adrenal slices. *Journal of Neuroscience* **17**, 2314-2323.

Nikolova, G., Jabs, N., Konstantinova, I., Domogatskaya, A., Tryggvason, K., Sorokin, L., Fassler, R., Gu, G. Q., Gerber, H. P., Ferrara, N. et al. (2006). The vascular basement membrane: A niche for insulin gene expression and beta cell proliferation. *Developmental Cell* **10**, 397-405.

Orci, L. (1976). Microanatomy of islets of Langerhans. *Metabolism-Clinical and Experimental* **25**, 1303-1313.

Orci, L., Thorens, B., Ravazzola, M. and Lodish, H. F. (1989). Localization of the pancreatic beta-cell glucose transporter to specific plasma-membrane domains. *Science* **245**, 295-297.

Paras, C. D., Qian, W. J., Lakey, J. R., Tan, W. H. and Kennedy, R. T. (2000). Localized exocytosis detected by spatially resolved amperometry in single pancreatic beta-cells. *Cell Biochemistry and Biophysics* **33**, 227-240.

Roignot, J., Peng, X. and Mostov, K. (2013). Polarity in Mammalian Epithelial Morphogenesis. *Cold Spring Harbor Perspectives in Biology* **5**.

Rutter, G. A., Loder, M. K. and Ravier, M. A. (2006). Rapid three-dimensional imaging of individual insulin release events by Nipkow disc confocal microscopy. *Biochemical Society Transactions* **34**, 675-678.

Singla, V. and Reiter, J. F. (2006). The primary cilium as the cell's antenna: Signaling at a sensory organelle. *Science* **313**, 629-633.

Sun, G., Tarasov, A. I., McGinty, J. A., French, P. M., McDonald, A., Leclerc, I. and Rutter, G. A. (2010). LKB1 deletion with the RIP2.Cre transgene modifies pancreatic beta-cell morphology and enhances insulin secretion in vivo. *American Journal of Physiology-Endocrinology and Metabolism* **298**, E1261-E1273.

Takahashi, N., Kishimoto, T., Nemoto, T., Kadowaki, T. and Kasai, H. (2002). Fusion pore dynamics and insulin granule exocytosis in the pancreatic islet. *Science* **297**, 1349-1352.

Thorens, B., Weir, G. C., Leahy, J. L., Lodish, H. F. and Bonnerweir, S. (1990). Reduced expression of the liver beta-cell glucose transporter isoform in glucose-insensitive pancreatic beta-

cells of diabetic rats. *Proceedings of the National Academy of Sciences of the United States of America* **87**, 6492-6496.

Thorn, P., Lawrie, A. M., Smith, P. M., Gallacher, D. V. and Petersen, O. H. (1993). Local and global cytosolic ca2+ oscillations in exocrine cells evoked by agonists and inositol trisphosphate *Cell* **74**, 661-668.

Wang, M. H., Li, J. X., Lim, G. E. and Johnson, J. D. (2013). Is Dynamic Autocrine Insulin Signaling Possible? A Mathematical Model Predicts Picomolar Concentrations of Extracellular Monomeric Insulin within Human Pancreatic Islets. *Plos One* **8**.

Weir, G. C. and Bonner-weir, S. (1990). Islets of langerhans - the puzzle of intraislet interactions and their relevance to diabetes. *Journal of Clinical Investigation* **85**, 983-987.

Yamamoto, M. and Kataoka, K. (1984). A comparative-study on the intercellular canalicular system and intercellular-junctions in the pancreatic-islets of some rodents. *Archivum Histologicum Japonicum* **47**, 485-493.

Yu, W., Datta, A., Leroy, P., O'Brien, L. E., Mak, G., Jou, T. S., Matlin, K. S., Mostov, K. E. and Zegers, M. M. P. (2005). beta 1-integrin orients epithelial polarity via Rac1 and laminin. *Molecular Biology of the Cell* **16**, 433-445.

Supplementary Material

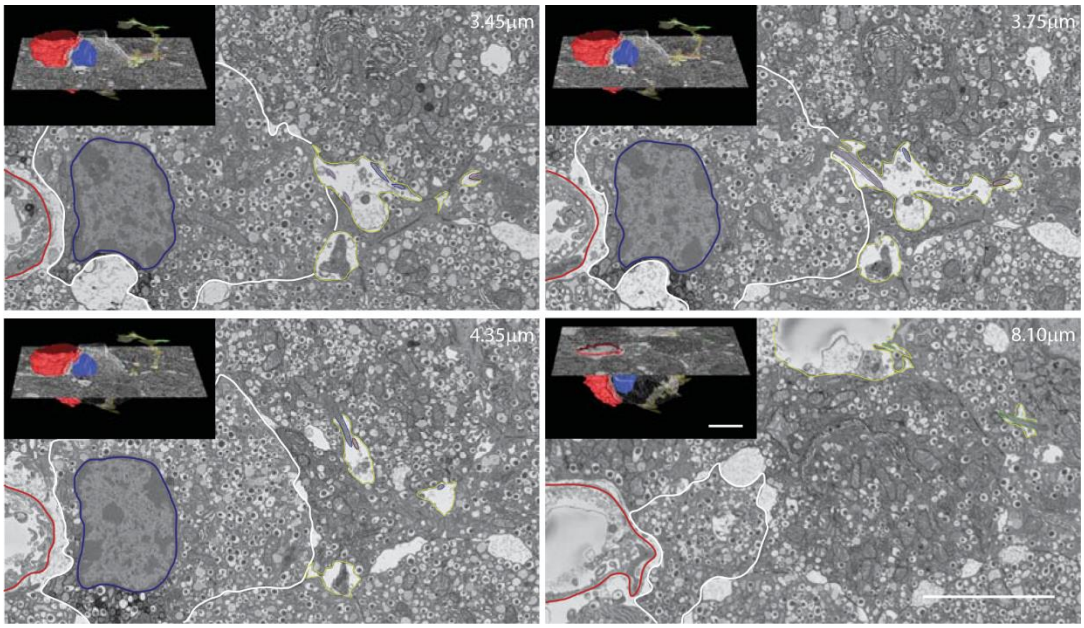

Fig. S1 **Four further examples of individual electron microscopy sections from the serial-section stack.** The IMOD outline shows the position of the nucleus (blue) cell (white), luminal space (yellow) and primary cilia (green, blue orange and purple). The Z location of each section is shown in the inserts.

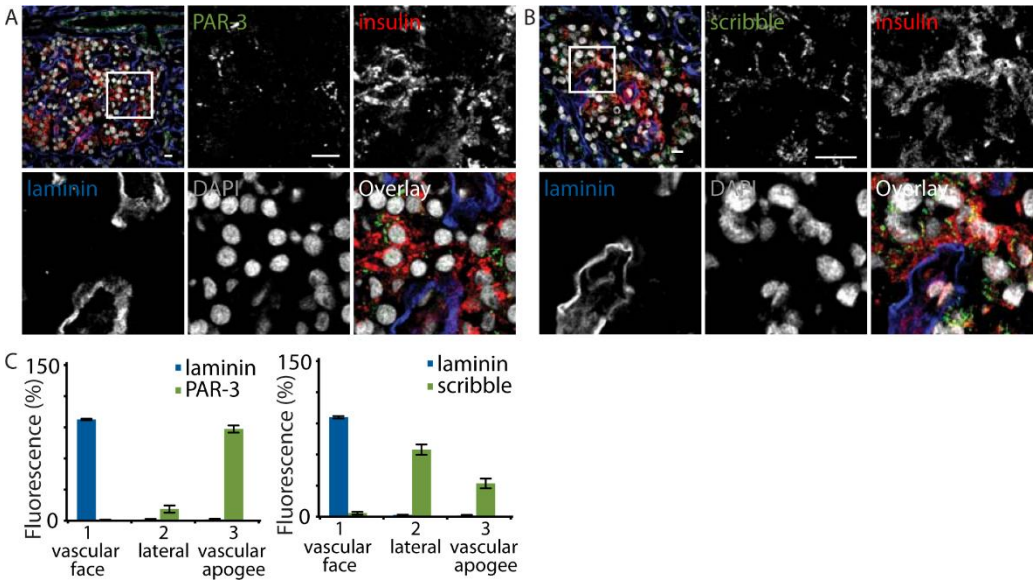

Fig. S2 **Human beta cells also have polarity determinants.** (A, C) PAR-3 and (B,C) scribble are enriched in similar domains to those of mouse beta cells.

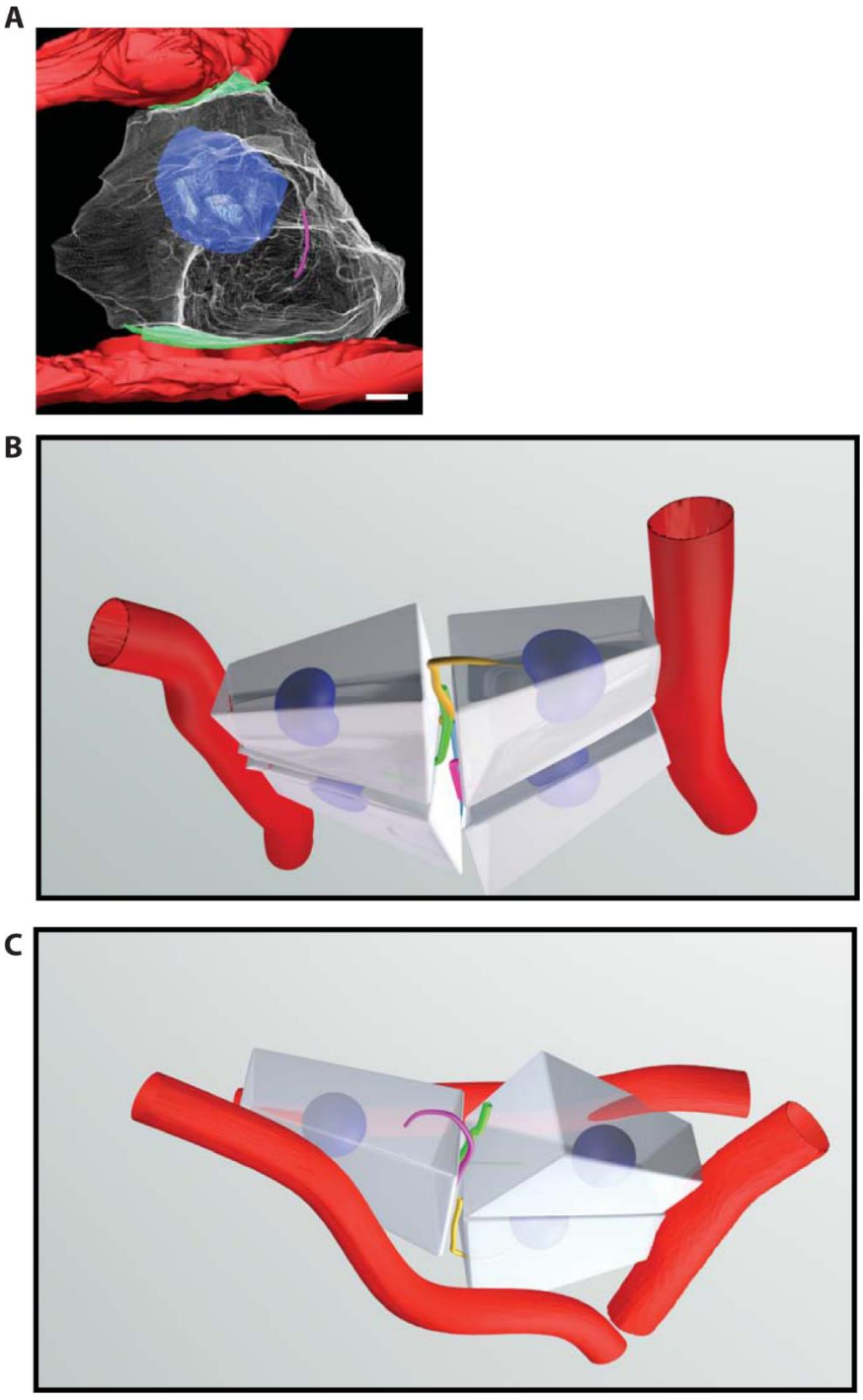

Fig. S3 **3D organisation of beta cells.** (A) re-analysis of the electron microscopy data of Fig. 1C show the primary cilia lies away from the two blood vessels. Scale 2 µm. (B and C) cartoon representations of the orientation of beta cells with one or two points of contact with blood vessels showing the primary cilia (yellow, green purple).

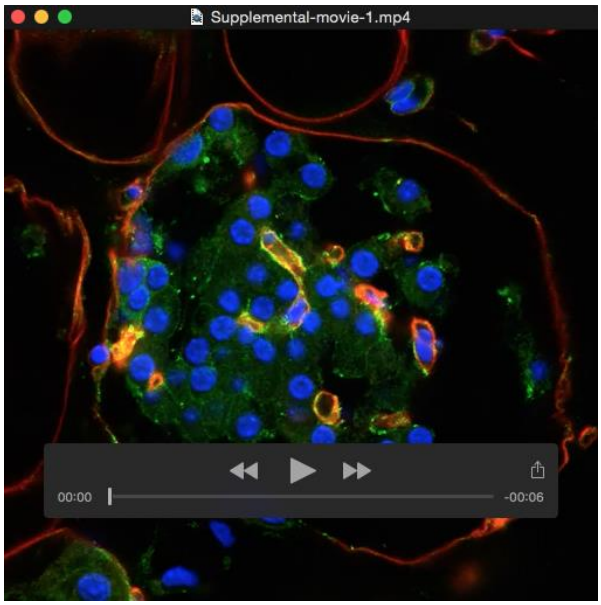

Movie 1. **Confocal image stack of liprin (green) and laminin (red) through an individual pancreatic islet of Langerhans.**

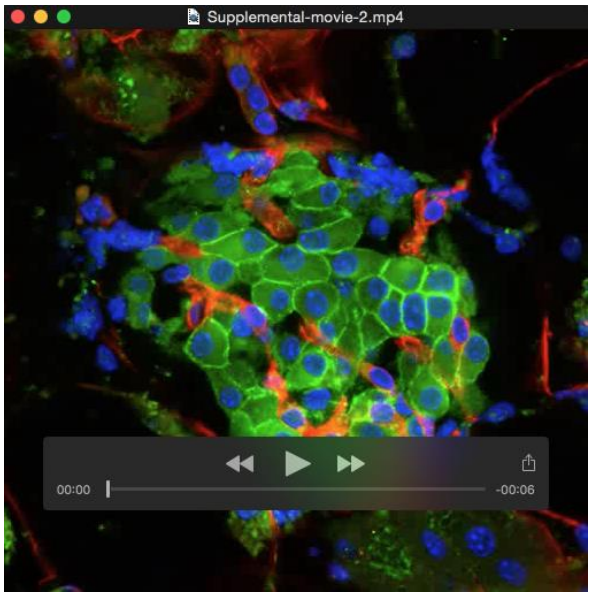

Movie 2. **Confocal image stack of GLUT2 (green) and laminin (red) through an individual pancreatic islet of Langerhans.**

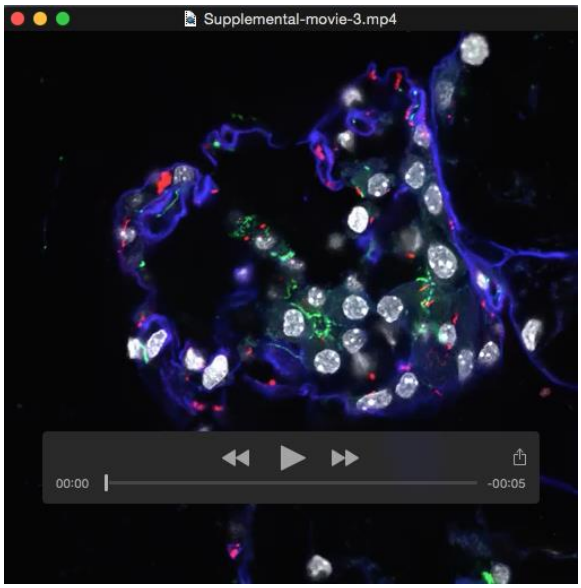

Movie 3. **Confocal image stack of ZO-1 (green) and acetylated tubulin (red) and laminin (blue) through an individual pancreatic islet of Langerhans.**

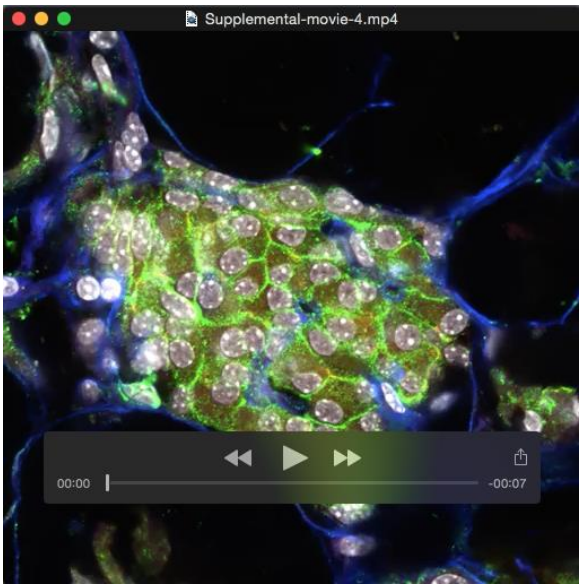

Movie 4. **Confocal image stack of PAR-3 (red) and E-cadherin (green) and laminin (blue) through an individual pancreatic islet of Langerhans.**

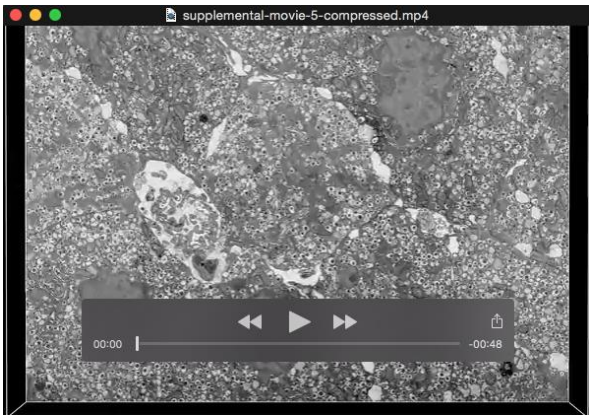

Movie 5. **3D image stack of serial electron micrograph sections through an islet highlighting the beta cell apical domain.**

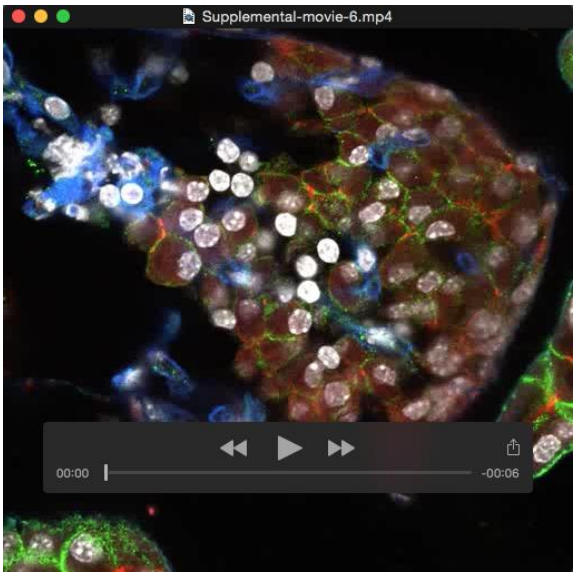

Movie 6. **Confocal image stack of PAR-3 (red) and Dlg (green) and laminin (blue) through an individual pancreatic islet of Langerhans.**

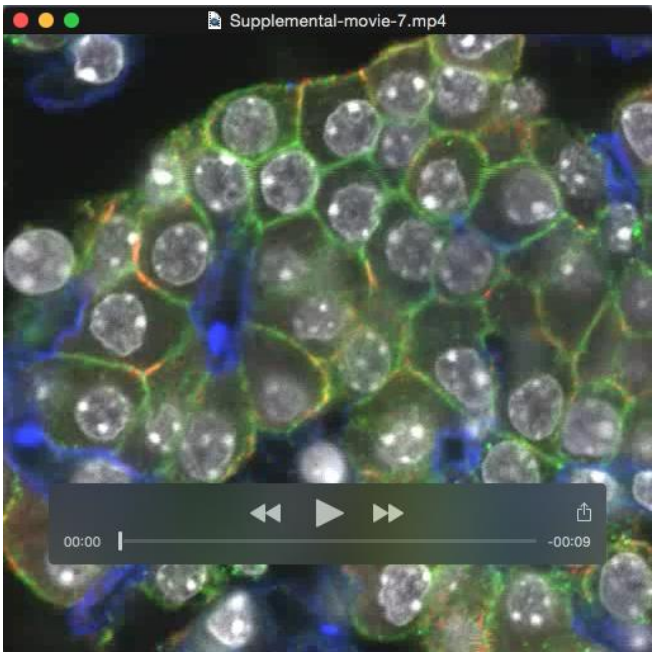

Movie 7. **Confocal image stack of PAR-3 (red) and scribble (green) and laminin (blue) through an individual pancreatic islet of Langerhans.**